Earthq Eng & Eng Vib (2016) 15: 425-433 **DOI**:10.1007/s11803-016-0333-1

Quasi-real time inversion method of three-dimensional epicenter coordinate, trigger time, and magnitude based on CORS

Xiao Dongsheng[1, 2†], Chang Ming[2‡], Su Yong[1‡], Hu Qijun[1†] and Yu Bing[1‡]

1. *School of Civil Engineering and Architecture, Southwest Petroleum University, Chengdu 610500, China*

2. *State Key Laboratory of Geohazard Prevention and Geoenvironment Protection, Chengdu University of Technology, Chengdu 610059, China*

Abstract: This study explores the quasi-real time inversion principle and precision estimation of three-dimensional coordinates of the epicenter, trigger time and magnitude of earthquakes with the aim to improve traditional methods, which are flawed due to missing information or distortion in the seismograph records. The epicenter, trigger time and magnitude from the Lushan earthquake are inverted and analyzed based on high-frequency GNSS data. The inversion results achieved a high precision, which are consistent with the data published by the China Earthquake Administration. Moreover, it has been proven that the inversion method has good theoretical value and excellent application prospects.

Keywords: continuous operation reference station (CORS); trigger time; three dimensional coordinate; magnitude; inversion

1 Introduction

Following an earthquake, a rapid assessment is made to determine the coordinates of the epicenter, trigger time, and magnitude, which all have great significance on emergency rescue and response, among other factors. Traditional assessment methods used to determine these three elements are made by broadband seismographs or accelerometers. However, for large earthquakes and/or near earthquakes, broadband seismographs may include saturation and tilt phenomenon, resulting in distortion of the record in terms of seismic wave speed and amplitude. The displacement obtained with accelerometers and two integral calculations of acceleration can also be distorted because of the phenomenon of tilting and rotating (Li, 2009; Li *et al*., 2015). Moreover, most of the scale of the magnitude is associated with the amplitude or frequency of the seismic wave. The larger vibration energies of the lower frequency part of a large earthquake are easy to lose in the seismograph record, which can lead to inaccurate assessments of these three earthquake elements, especially for earthquakes that are greater than M_s 8.0 (Allen and Hiroo, 2003).

Correspondence to: Chang Ming, State Key Laboratory of Geohazard Prevention and Geoenvironment Protection, Chengdu University of Technology, Chengdu 610059, China
Tel: +86-28-83037621
E-mail: changmxq@126.com
†Associate Professor; ‡Lecturer

Supported by: National Natural Science Foundation under Grant No. 51574201, Opening Fund of State Key Laboratory of Geohazard Prevention and Geoenvironment Protection (Chengdu University of Technology) under Grant No. SKLGP2016K017, Open Research Fund by Sichuan Engineering Research Center for Emergency Mapping & Disaster Reduction under Grant No.K2015B008, The State Administration of Work Safety under Grant No. 2014_3335, Soft Science Research Projects in Sichuan Province under Grant No. 2015zr0049

Received July 24, 2015; **Accepted** November 16, 2015

2 Inversion method for the elements of the earthquake

2.1 Inversion of three-dimensional coordinates of the epicenter and trigger time

The deducing process of the inversion method is used by the indirect adjustment method based on the least-square theory, that is,

$$\sum_{i=1}^{n} q_i v_i^2 = \min \tag{1}$$

where $q_i = f(d_i)$ is the weight function related to epicentral distance; and v_i is the correction of the three elements of the earthquake, that is,

$$v_i = \sqrt{(N_i - \hat{N}_0)^2 + (E_i - \hat{E}_0)^2 + (H_i - \hat{H}_0)^2} - U(t_i - \hat{T}_0) \tag{2}$$

where $(\hat{N}_0, \hat{E}_0, \hat{H}_0, \hat{T}_0)$ are estimates of the elements of the earthquake; (N_i, E_i, H_i, t_i) are geodetic coordinates of the No. i CORS station; U is the propagation speed of the P wave; t_i is the arrival time of the P wave on the No. i CORS; and T_0 is the trigger time of the P wave on

the epicenter (Surveying adjustment subject groups of Wuhan University, 2002).

$$\hat{N}_0 = N_0 + n,\ \hat{E}_0 = E_0 + e,\ \hat{H}_0 = H_0 + h,\ \hat{T}_0 = T_0 + t \tag{3}$$

where (N_0, E_0, H_0, T_0) are the approximate values of $(\hat{N}_0, \hat{E}_0, \hat{H}_0, \hat{T}_0)$, respectively. The matrix form of Eq. (3) is as follows:

$$\begin{bmatrix} \hat{N}_0 \\ \hat{E}_0 \\ \hat{H}_0 \\ \hat{T}_0 \end{bmatrix} = \begin{bmatrix} N_0 \\ E_0 \\ H_0 \\ T_0 \end{bmatrix} + \begin{bmatrix} n \\ e \\ h \\ t \end{bmatrix} \tag{4}$$

The simplification of Eq. (4) is written into Eq. (5):

$$\hat{\boldsymbol{X}} = \boldsymbol{X}^0 + \boldsymbol{x} \tag{5}$$

$$\hat{\boldsymbol{X}} = \begin{bmatrix} \hat{N}_0 \\ \hat{E}_0 \\ \hat{H}_0 \\ \hat{T}_0 \end{bmatrix} \quad \boldsymbol{X}^0 = \begin{bmatrix} N_0 \\ E_0 \\ H_0 \\ T_0 \end{bmatrix} \quad \boldsymbol{x} = \begin{bmatrix} n \\ e \\ h \\ t \end{bmatrix} \tag{6}$$

Equation (7) can be deduced from the linearization of Eqs. (3), (4), (5) and Eq. (6) to Eq. (2).

$$v_i = -\frac{\Delta N_{i0}^0}{d_{i0}^o} \cdot n - \frac{\Delta E_{i0}^0}{d_{i0}^o} \cdot e - \frac{\Delta H_{i0}^0}{d_{i0}^o} \cdot h - Ut_i + UT_0 + Ut + \sqrt{(N_i - N_0)^2 + (E_i - E_0)^2 + (H_i - H_0)^2} \tag{7}$$

where there are $\Delta N_{i0}^0 = N_0 - N_i$, $\Delta E_{i0}^0 = E_0 - E_i$, $\Delta H_{i0}^0 = H_0 - H_i$, Eq. (7) is simplified as follows:

$$v_i = -\frac{\Delta N_{i0}^0}{d_{i0}^o} \cdot n - \frac{\Delta E_{i0}^0}{d_{i0}^o} \cdot e - \frac{\Delta H_{i0}^0}{d_{i0}^o} \cdot h + Ut - l \tag{8}$$

where there is

$$l = -(-Ut_i + UT_0 + \sqrt{(N_i - N_0)^2 + (E_i - E_0)^2 + (H_i - H_0)^2})$$

Hypothesis: $L_i = -\frac{\Delta N_{i0}^0}{d_{i0}^o}$, $M_i = -\frac{\Delta N_{i0}^0}{d_{i0}^o}$, $R_i = -\frac{\Delta H_{i0}^0}{d_{i0}^o}$

Eq. (8) is transformed into Eq. (9):

$$v_i = -L_i \cdot n - M_i \cdot e - R_i \cdot h + Ut - l \tag{9}$$

Equation (9) is the error equation of the CORS i, when the number of the CORS stations is r. The matrix of the equations is written as follows (Surveying adjustment subject groups of Wuhan University, 2002):

$$\boldsymbol{V} = \boldsymbol{Bx} - \boldsymbol{l} \tag{10}$$

where there are,

$$\boldsymbol{V} = \begin{bmatrix} v_1 \\ v_2 \\ \cdots \\ v_r \end{bmatrix} \quad \boldsymbol{x} = \begin{bmatrix} n \\ e \\ h \\ t \end{bmatrix} \quad \boldsymbol{l} = \begin{bmatrix} l_1 \\ l_2 \\ \cdots \\ l_r \end{bmatrix} \tag{11}$$

$$\boldsymbol{B} = \begin{bmatrix} L_1 & M_1 & R_1 & U \\ L_2 & M_2 & R_2 & U \\ . & . & . & . \\ L_r & M_r & R_r & U \end{bmatrix} \quad \boldsymbol{Q} = \begin{bmatrix} q_{\hat{N}} & & .. & .. \\ . & q_{\hat{E}} & & . \\ . & . & q_{\hat{H}} & . \\ .. & .. & & q_{\hat{U}} \end{bmatrix} \tag{12}$$

$\boldsymbol{V}^{\mathrm{T}}\boldsymbol{QV} = \min$ is the matrix form of $\sum_{i=1}^{n} q_i v_i^2 = \min$, because r parameters are independent, so $\boldsymbol{x}$ can be solved according to the free extremum method, which is expressed as follows:

$$\frac{\partial \boldsymbol{V}^{\mathrm{T}}\boldsymbol{QV}}{\partial x} = 2\boldsymbol{V}^{\mathrm{T}}\boldsymbol{Q}\frac{\partial \boldsymbol{V}}{\partial x} = \boldsymbol{V}^{\mathrm{T}}\boldsymbol{QB} = 0 \tag{13}$$

Make the matrix transposition between two sides of $\boldsymbol{V}^{\mathrm{T}}\boldsymbol{QB} = 0$, which is written as follows:

$$\boldsymbol{B}^{\mathrm{T}}\boldsymbol{QV} = 0 \tag{14}$$

Put Eq. (10) into Eq. (14), which is written as follows:

$$\boldsymbol{B}^{\mathrm{T}}\boldsymbol{QBx} - \boldsymbol{B}^{\mathrm{T}}\boldsymbol{Ql} = 0 \tag{15}$$

According to Eq. (15), $\boldsymbol{x}$ is solved, which is as follows:

$$\boldsymbol{x} = [\boldsymbol{B}^{\mathrm{T}}\boldsymbol{QB}]^{-}\boldsymbol{B}^{\mathrm{T}}\boldsymbol{Ql} \tag{16}$$

Put Eq. (16) into Eq. (4), the values of $(\hat{N}_0, \hat{E}_0, \hat{H}_0, \hat{T}_0)$ are solved (Zumberge *et al*., 1997).

2.2 Estimation of depth of hypocenter

The depth of the hypocenter is part of the epicenter location, and is as follows:

$$\Delta H = H - \hat{H}_0 \tag{17}$$

where ΔH is the depth of the hypocenter, and H is the ground elevation of the epicenter.

2.3 Accuracy estimation

The above studies explain that $(\hat{N}_0, \hat{E}_0, \hat{H}_0, \hat{T}_0)$ are four unknown variables, and need data from two CORS stations. When the number of CORS stations exceeds two, it is shown that there must be a redundant observation quantity, and the number is re; the accuracy

evaluation is then as follows (Surveying adjustment subject groups of Wuhan University, 2002).

(1) Error estimation of unit weight is as follows:

$$\hat{\sigma}_0 = \sqrt{\frac{\partial \boldsymbol{V}^{\mathrm{T}} \boldsymbol{Q} \boldsymbol{V}}{\mathrm{re}}} \tag{18}$$

(2) Error estimation of the parameters.

According to the indirect adjustment method, $[\boldsymbol{B}^{\mathrm{T}}\boldsymbol{Q}\boldsymbol{B}]^{-}$ is the weight reciprocal matrix of the parameters, which are independent of each other. Therefore, the weight reciprocal is expressed in the following diagonal matrix:

$$[\boldsymbol{B}^{\mathrm{T}}\boldsymbol{Q}\boldsymbol{B}]^{-} = \begin{bmatrix} W_{N_0} & \cdots & \cdots & \cdots \\ \cdot & W_{E_0} & & \cdot \\ \cdot & & W_{H_0} & \cdot \\ \cdots & \cdots & \cdots & W_{T_0} \end{bmatrix} \tag{19}$$

From $\hat{\sigma}_i = \hat{\sigma}_0 W_i$, the error estimation of the matrix is as follows:

$$\begin{bmatrix} \hat{\sigma}_{N_0} \\ \hat{\sigma}_{E_0} \\ \hat{\sigma}_{H_0} \\ \hat{\sigma}_{T_0} \end{bmatrix} = \begin{bmatrix} \hat{\sigma}_0 W_{N_0} \\ \hat{\sigma}_0 W_{E_0} \\ \hat{\sigma}_0 W_{H_0} \\ \hat{\sigma}_0 W_{T_0} \end{bmatrix} \tag{20}$$

Two times the error are taken as the actual error, and is written as:

$$\mathrm{Error} = 2\hat{\sigma}_i \qquad (\hat{\sigma}_i : \hat{\sigma}_{N_0}, \hat{\sigma}_{E_0}, \hat{\sigma}_{H_0}, \hat{\sigma}_{T_0}) \tag{21}$$

2.4 Magnitude estimation

In 1945, Gutenberg recorded different seismic data in California by several strong-motion seismographs. He applied the empirical regression method to deduce the level peak displacement of the station, and the relationship between the epicentral distance and magnitude, to develop a magnitude estimation model (Blewitt *et al*., 2006; Fang *et al*., 2014; Wu and Li, 2006; Wright *et al*., 2012), as follows (Surveying adjustment subject groups of Wuhan University, 2002):

$$M_{\mathrm{s}} = \log(A) + 1.656\log(d_i) + 1.818 \tag{22}$$

where A is the level peak displacement caused by the seismic surface wave, whose unit is μm; d_i ($20^0 < d_i < 130^0$) is the epicentral distance, whose unit is degree (1° is 100 km); and M_{s} is the magnitude.

Magnitude estimation is related to the distance from the epicenter, because the closer the CORS station is to the epicenter, the larger the influence of the CORS signal, so the reliability of the result is much lower. Therefore, the weight function can be expressed with distances (Wu and Li, 2006); the weighted estimation of the magnitude is as follows:

$$q_i(d_i) = d_i \tag{23}$$

$$M_s = \frac{\sum_{i=1}^{n} q_i M_{\mathrm{S}i}}{\sum_{i=1}^{n} q_i} \tag{24}$$

where $M_{\mathrm{S}i}$ is the magnitude of every CORS station, and $q_i = f(d_i)$ is the weight function related to epicentral distance.

3 Inversion method applied in the Lushan earthquake based on CORS

3.1 Geographical and geological background in Lushan

Lushan is in the Longmenshan fault zone, and the Longmenshan fault zone, located in the mid-eastern boundary of the Tibetan plateau, is situated between the Tibetan plateau and the Sichuan basin. The Longmenshan fault zone is surrounded by the southern margin of the Qinling fault zone and the Xianshuihe fault zone. It originates from the area of Guangyuan and Baishui, after intersecting with the east-west tectonic belt of Kunlun-Qinling at an oblique angle, expanding to the southwest along the west boundary of the Sichuan Basin, and it finally meets at the north-south tectonic belt of Kangding and the northwest fault zone of Xianshuihe. The length of the Longmenshan fault zone is about 500 km, and its width is about 70 km. The Longmenshan fault zone is composed of three large fault zones from south to north: Wenchuan-Maoxian-Pingwu-Qingchuan shown as F_1 in Fig. 1, Yingxiu-Beichuan-Guanzhuang shown as F_2 in Fig. 1, and Dujiangyan-Hanwang-Anxian shown as F_3 in Fig. 1 (Peng *et al*., 2009).

3.2 CORS monitoring points in Longmen region of CORS network

The GNSS data are derived from the CORS network of the Sichuan province. The network are mainly distributed in the Sichuan basin, covering an area of 250,000 km^2, and its scientific research is mainly based on monitoring crustal movement. Until April 2013, the number of CORS stations distribution in Sichuan and the surrounding areas was approximately 70 or so, as shown in Fig. 2 (Li, 2009).

Based on these observations, in order to reduce the influence of atmospheric delay and ionospheric delay, the closer the optimal selection of the reference stations (< 10 km), the better the effect. When applied in a coseismic crustal deformation study, the reference

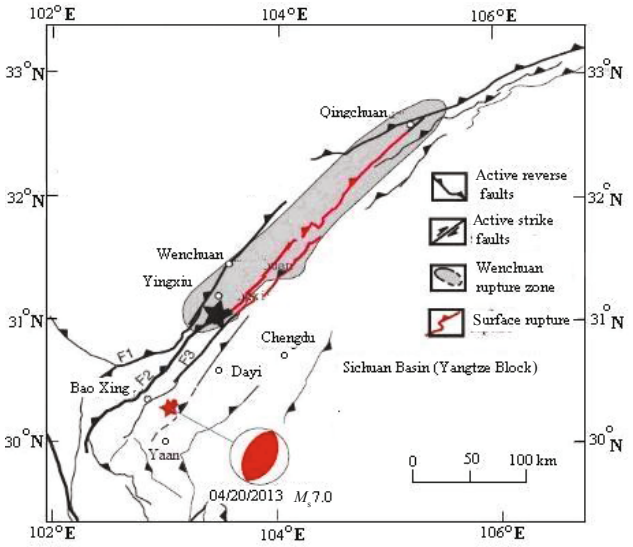

Fig. 1 Geological background of the Sichuan Basin (Peng *et al*., 2009). Longitudinal axis is longitude; transverse axis is latitude. The black star is the epicenter of Wenchuan earthquake, located in Yinxiu Town of Wenchuan County. The red star is the epicenter of Lushan earthquake, located in Ya'an City. Chengdu is the capital of Sichuan and is located in the Sichuan Basin

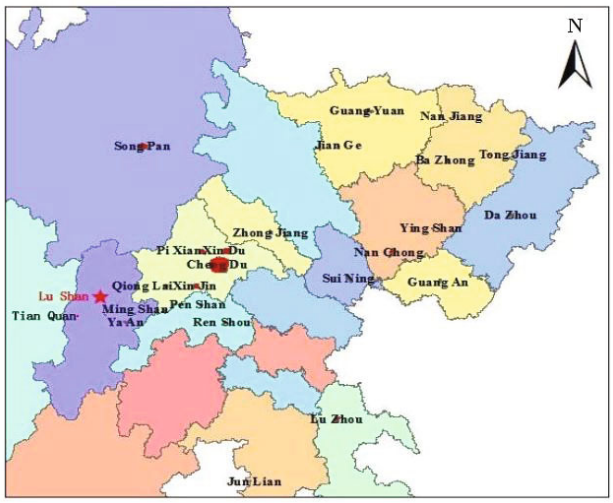

Fig. 2 CORS stations distribution in Lushan region

stations should be kept away from the seismic belt, and the seismic active region. After the earthquake, seismic waves spread very fast. If the selection of the reference stations is too close, the program calculation is set for stationary, and no displacement occurs, the calculated results for the displacement of the moving station may be the result of superposition of the reference station and the moving station's displacement, not the actual motion state of the moving station, so that it is unable to detect the station's movements (Yin *et al*., 2010, 2009; Bilich *et al*., 2008). Two options are available to solve this problem as follows: use the theory of seismic propagation distance, and choose the station that is farthest from the moving station as a reference for the calculation, or use the method of wire transfer from the nearest to the farthest station (Gu *et al*., 2015).

Choosing the station that has a distance greater than the product of the seismic wave propagation velocity and duration as a reference station can achieve a relatively reliable positioning result. In an inland earthquake, the survey results could be significant if the Qionglai station, which is the nearest to the Ya'an station, is chosen as the reference station. The Zhongjiang station in GNSS sequence of 237-277 s obviously contained its own set of movements when the earthquake occurred (Li, 2009). If the aim is to have the reference station after selection reflect the full movement in the station, and to achieve high precision at the same time, the Penshan station is the best in theory. However, in practice, because of the observation quality, the Jiange station is actually the best choice. In the figure above, the Qionglai station is used as the reference station to analyze the movement of the Ya'an station, since it is important to determine whether the seismic wave arrived first at the Ya'an or Qionglai stations. Comparing the sequence where the Qionglai station is the reference station with the others, if the jump moment of the seismic wave is in line with other stations, it is seen that the seismic wave first arrived at the Ya'an station. On the contrary, if the jump happened earlier than at the other stations, it is seen that the seismic wave first arrived at the Qionglai station. In the E–W direction of the sequence diagram, the time that the Qionglai station jumps is faster than at the other stations at about 1.5 s, and the arrival time is about 192.1 s by determination. The coordinates of the timing in the N–S direction is consistent with the other stations, and it takes 190.9 s to arrive. The main cause of this phenomenon is that the Ya'an station in the east-west direction is not sensitive to the arrival of the seismic waves (Fang, 2010; Yin *et al*., 2010; Meng *et al*., 2007).

4 Inversion implementation of three-dimensional epicenter coordinate and trigger time

Through the inversion method described above, the determination of the arrival moment of the seismic wave at the CORS station is a key step, and makes $\Delta t = t_i - T_0$ known. Second, via the distance ($U\Delta t$) rendezvous, approximation of the epicenter location and trigger time is obtained according to the inversion method, which provides an estimate. The details are discussed in detail later.

4.1 Choice of characteristic function

Past research shows that in the role of uniform shear stress, due to expansion at a constant speed circular

crack, the expansion of the circular crack at a constant speed lead to a step change of the displacement (Sato and Hirasawa, 1973). Through the characteristic function, these features were enlarged as far as possible so as to protrude, and pick up.

S transformation is a kind of nondestructive reversible linear time-frequency analysis method. It combines short-time Fourier transform with wavelet transform, and not only keeps the direct relationship with the Fourier transform, but also has different resolutions under different frequencies (Stockwell, 2007; Stockwell *et al*., 1996; Zhang *et al*., 2012, Yi *et al*., 2008). Assuming a continuous time series function $h(t)$, the *S* transformation is expressed as:

$$S(\tau, f)=\int_{-\infty}^{\infty} h(t)\frac{|f|}{\sqrt{2\pi}}\exp(\frac{-f^2(\tau-t)^2}{2})\exp(-2\pi ift)\mathrm{d}\tau \tag{25}$$

where $h(t)$ is the original coordinate sequence, $\frac{|f|}{\sqrt{2\pi}}\exp(\frac{-f^2(\tau-t)^2}{2})$ is the Gauss window function, t is the time, f is the frequency, and τ is the scale factor that controls the Gauss window in the t axis position.

4.2 Determination of the arrival time of P wave

The TRACK module in GAMIT is used to process the HF GNSS data (http://www-gpsg.mit.edu/~simon/gtgk/). TRACK is a high precision GNSS data processing software developed by the Massachusetts Institute of Technology and Scripps Institute of Oceanography. The kinematic positioning module in GAMIT/GLOBK can be used to account for high frequency GNSS data (Simona *et al*., 2013; Hung and Rau, 2013). From the 0.02 s of sampling frequency (Liu *et al*., 2013), according to the *S* transformation of the time-series of the coordinates at the Qionglai and Ya'an stations, and the spectrum diagram of the displacement mutation caused by the earthquake, determination of the arrival time of the seismic wave at the CORS station is obtained as follows (Zhang *et al*., 2012):

From existing data, it is seen that the first arrival time of the seismic wave is not consistent in the N–S and E–W directions, which is related to the wave movement at these stations and the error assessment in the *S* transform. In order to further compare and distinguish the first arrival time of the seismic wave, the acceleration of the horizontal displacement for $\mathrm{d}s=\sqrt{(\mathrm{d}\psi(N_0))^2+(\mathrm{d}\varphi(E_0))^2}$ ($\psi(N_0)$ and $\varphi(E_0)$,

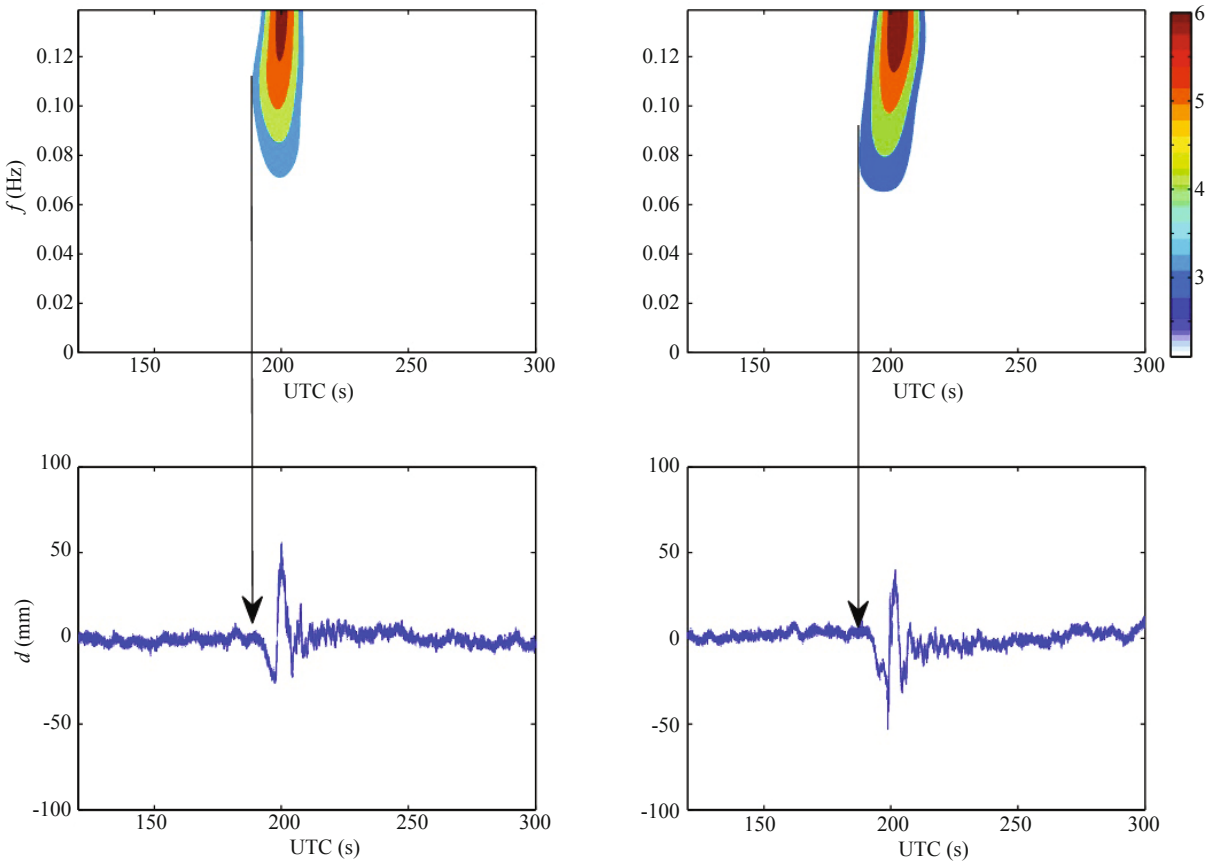

Fig. 3 Displacement spectrum of Qionglai, the black arrow point to the mutation moment for earthquake, namely the arrival time of seismic wave (Li, 2009)

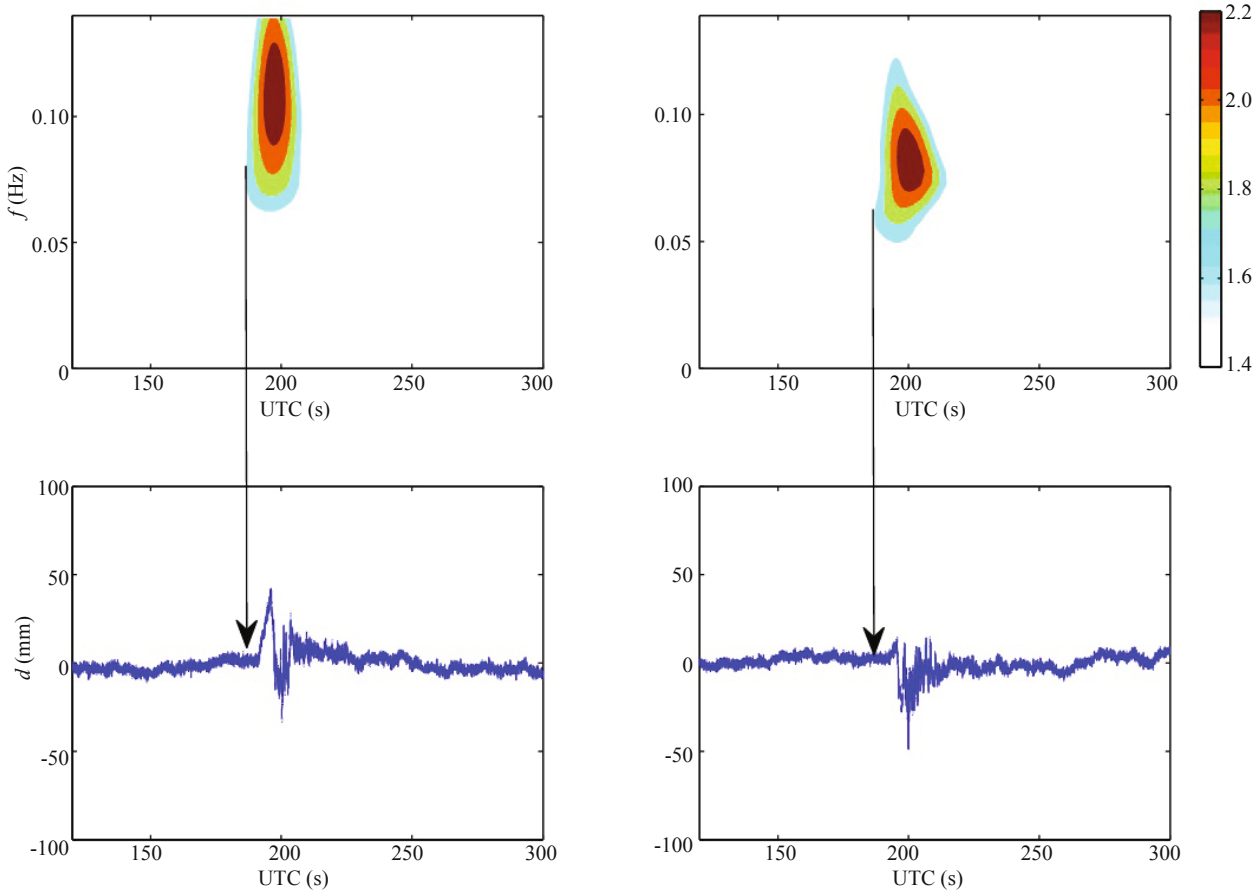

Fig. 4 Displacement spectrum of Ya'an, the black arrow point to the mutation moment for earthquake, namely the arrival time of seismic wave (Li, 2009)

respectively, are the corresponding plane rectangular coordinate of (N_0, E_0) and should also be in the course of the S transform, which is a key condition of the calculation in the three-dimensional coordinate of the epicenter. The first arrival time of the seismic wave, namely the displacement mutation moment caused by the arrival of the seismic wave at the CORS station, is shown in Table 1 (Crowell *et al*., 2013; Xu *et al*., 2010; Wu *et al*., 2013).

There was an obvious time difference between the Ya'an station, where the seismic wave first arrived, and the others, and it was 26 s different from the Chengdu station. The time interval was short and very important. In disaster relief and seismic emergency response, a rapid seismic pre-alarm would likely save lives. Therefore, it is important to study seismic waves at increased epicentral distances, and seismic wave energy attenuation. The P seismic wave arrived first at the CORS station; while in theory, it should have been the P wave (Gu *et al*., 2015;Wu *et al*., 2013; Wang, *et al*., 2013;Wang, *et al*., 2000;Yin *et al*., 2010).

4.3 Inversion of epicenter location, depth of hypocenter and trigger time

Three stations were analyzed, the Ya'an, Tianquan and Qionglai stations, which are where the seismic waves arrived first. The seismic waves reached these stations at speeds of 7.11 km/s, 7.02 km/s, 7.01 km/s, respectively, with an average speed of 7.05 km/s, which corresponds to the characteristics of the speed of the P wave. Centered on Ya'an station where the seismic wave arrived first, the epicenter was 30.04N,103.05E, and its precision was 0.01°. The difference in the epicenter published by the China Earthquake Administration was -0.24° in the N–S direction and 0.14° in the E–W direction (Gu *et al*., 2015; Li, 2009).

By inversion, the depth of the hypocenter was 16.7 km, with an error and relative error of 3.7 and 0.22 km, respectively. The trigger time was 183.71 s in GNSS time, and minus 16 s of the jump time from 1982, and was then converted to 8:02:47.71 in Beijing time, with an error and relative error of 0.04, 0.00024 s, respectively. In general, the inversion was ideal, and the remaining errors may be related to the time of the seismic wave arrival extracted by the spectrum (Gu *et al*., 2015; Li, 2009).

5 Weighted estimation of magnitude

The magnitude issued by the China Earthquake Administration was M_s 7.0, according to different epicentral distances of the CORS station; thus, different

methods were used in this study. From Table 2, the CORS stations is divided into three types: (1) epicentral distance of the CORS station was less than 1°, (2) regardless of the epicentral distance, the arithmetic average of magnitude of the CORS was obtained; and (3) considering the difference between the epicentral distance and the condition ($20^o < d_i < 130^o$) in Eq. (22), the weighted average magnitude of CORS was solved as shown in Table 3 (Gu *et al*., 2015).

It is observed that the Qionglai, Tianquan and Ya'an stations are closer to the epicenter and are affected by the earthquake so as to enlarge the error, and it is seen that the magnitude obtained by the weighted average method is closer to the magnitude published by China Earthquake Administration, which shows that the method described herein is better than the other methods.

6 Conclusion

In this study, the inversion method of three elements of an earthquake is set up, with reference to the existing seismic data, to better analyze and explain the inversion process. The results are as follows:

(1) An inversion method was established for three-dimensional epicenter coordinates, trigger time, and magnitude based on CORS, and was successfully applied to the Lushan earthquake.

(2) The real time and high precision positioning of the CORS station enabled access to the quasi-real time condition of the three elements, which ensured the precision of the three inversion elements.

(3) The characteristic function was optimized to improve the accuracy of the selection speed or acceleration mutation to accurately determine the arrival moment of the seismic wave.

Acknowledgement

The authors express their appreciation to Professor Huang Dinghua for providing detailed assistance. We also

Table 1 Time of seismic wave arrival from epicenter to CORS station

Station	Time of acceleration mutation (s)		
	N–S direction	E–W direction	Average
Chengdu	217.74	216.02	216.88
Qionglai	193.22	192.24	192.73
Tianquan	191.34	193.28	192.31
Ya'an	190.98	190.52	190.75

Table 2 Estimation of magnitude

CORS station	Epicentral distance (km)	Weight $q_i(d_i)=d_i$	Magnitude M_{si}	CORS station	Epicentral distance (km)	Weight $q_i(d_i)=d_i$	Magnitude M_{si}
Qionlai	30	30	5.82	Xindu	229	229	6.86
Tianquan	34	34	5.83	Suining	247	247	6.94
Ya'an	35	35	5.82	Penshan	264	264	6.89
Xinjin	98	98	6.21	Songpan	267	267	6.97
Pixian	99	99	6.35	Julian	278	278	6.96
Renshou	107	107	6.26	Luzhou	282	282	7.01
Chengdu	109	109	6.44	Nanchong	286	286	6.97
Zhongjiang	167	167	6.6	Jiange	323	323	7.08
Mingshan	173	173	6.67	Guangyuan	360	360	7.14
Yingshan	189	189	6.71	Bazhong	396	396	7.19

Table 3 Comparison of magnitude evaluation

Epicentral distance (1°= 100 km)	Magnitude estimation	Magnitude issued by China Earthquake Administration	Error	Relative error
$d_i \le 1^o, q_i(d_i)=1$	6.32	M_s7.0	0.68	9.7%
$d_i < 130^o, q_i(d_i)=1$	6.77		0.23	3.3%
$20 < d_i < 130^o, q_i(d_i)=d_i$	7.01		0.11	1.6%

thank two anonymous reviewers for their constructive comments to improve the manuscript. This research was supported by the National Natural Science Foundation of China under Grant No. 51574201, Opening Fund of State Key Laboratory of Geohazard Prevention and Geoenvironment Protection (Chengdu University of Technology), Open Research Fund by Sichuan Engineering Research Center for Emergency Mapping & Disaster Reduction under Grant No. K2015B008, The State Administration of Work Safety under Grant No. 2014_3335, and Soft Science Research Projects in Sichuan Province under Grant No. 2015zr0049.

References

Allen RM and Hiroo K (2003), "The Potential for Earthquake Early Warning in Southern California," *Translated World Seismology*, **300**(5620): 786–789. (in Chinese)

Bilich A, Cassidy JF and Larson KM (2008), "GPS Seismology: Application to the 2002 M_w7.9 Denali Fault Earthquake," *Bulletin of the Seismological Society of America*, **98(**2): 593–606.

Blewitt G, Kreemer C, Hammond WC, *et al*. (2006), "Rapid Determination of Earthquake Magnitude Using GPS for Tsunami Warning Systems," *Geophysical Research Letters*, **33**(11): 431–433.

Crowell BW, Bock Y and Squibb MB (2013), "Demonstration of Earthquake Early Warning Using Total Displacement Wave Forms from Real-time GPS Networks," *Seismol Res Lett*, **80**(5): 772–782.

Fang RX (2010), "High-rate GPS Data Non-difference Precise Processing and Its Application on Seismology," *PhD Dissertation*, Wuhan University. (in Chinese)

Fang RX, Shi C,Wang G, *et al*. (2014), "Determination of Earthquake Magnitude Using GPS Displacement Waveforms from Real-time Precise Point Positioning," *Geophysical Journal International*, **196**(1): 461–472.

Gu T, Li M, Chen C, *et al*. (2015), "The Lushan Earthquake Characteristic Analysis Based on High-rate GPS," *Science Technology and Engineering*, **15**(16): 128–131. (in Chinese)

Hung HK and Rau RJ (2013), "Surface Waves of the 2011 Tohoku Earthquake: Observations of Taiwan's Dense High-rate GPS Network," *Journal of Geophysical Research: Solid Earth*, **118**(1): 32–345.

Li M (2009), "Time-varying Displacement Field Mapping and Earthquake Three Elements Inversion Using CORS Network Measurements," *PhD Dissertation*, Southwest Jiaotong University. (in Chinese)

Li M, Huang DF, Yan L, *et al*. (2015), "Quasi-real Time Determination of 2013 M_w 6.6 Lushan Earthquake Epicenter, Trigger Time and Magnitude Using 50 Hz GPS Observations," *China Satellite Navigation Conference*, **3**(1): 27–30. (in Chinese)

Liu G, Zhao B, Zhang R, *et al*. (2013), "Near-field Surface Deformation During the April 20, 2013, M_s7.0 Lushan Earthquake Measured by 1-HZ GNSS," *Journal of Geodesy and Geodynamics*, **4**(2): 1–5.

Meng GJ, Ren JW, Jin HL, *et al*. (2007), "Data Processing Methods of High-rate GPS and Its Application to Seismology," *Recent Developments in World Seismology*, **343**(7): 26–31. (in Chinese)

Peng H, Ma XM and Jiang JJ (2009), "Stability and Stress Measurement Near the Qingchuan Fault in the Northern Lingmen Mountains," *Journal of Geomechanics*, **15**(2): 116–118.

Sato T and Hirasawa T (1973), "Body Wave Spectra from Propagating Shear Cracks," *J. Phys. Earth*, **21**: 415–431.

Simona C, Allen RM and Aldo Z (2013), "Application of Real-time GPS to Earthquake Early Warning in Subduction and Strike-slip Environments," *Journal of Geophysical Research Solid Earth*, **118**(7): 3448–3461.

Stockwell RG (2007), "A Basis for Efficient Representation of the *S*-transform," *Digital Signal Processing*, **17**(1): 371–393.

Stockwell RG, Mansinha L and Lowe RP (1996), "Localisation of the Complex Spectrum: the S Transform," *Journal of Association of Exploration Geophysicists*, **17**(3): 99–114.

Surveying Adjustment Subject Groups of Wuhan University (2002), "Error Theory Theory and Surveying Adjustment," *Wuhan University Press*, PP. 22–281. (in Chinese)

Wang SY, Yu YX, Gao AJ, *et al*. (2000), "Development of Attenuation Relations for Ground Motion in China," *Earthquake Research in China*, **16**(2): 99–106. (in Chinese)

Wang YS, Li XJ and Zhou ZH (2013), "Research on Attenuation Relationships for Horizontal Strong Ground Motions in Sichuan-Yunnan Region," *Acta Seismologica Sinica*, **35**(2): 238–249. (in Chinese)

Wright TJ, Houlié N, Hildyard M, *et al*. (2012), "Real-time, Reliable Magnitudes for Large Earthquakes from 1Hz GPS Precise Point Positioning: The 2011 Tohoku-Oki (Japan) Earthquake," *Geophysical Research Letters*, **39**(12): 229–240.

Wu YM and Li Z (2006), "Magnitude Estimation Using the First Three Seconds P-wave Amplitude in Earthquake Early Warning," *Geophysical Research Letters*, **33**(16): 271–284.

Wu YQ, Jiang ZS, Wang M, *et al*. (2013), "Preliminary Results Pertaining to Coseismic Displacement and Preseismic Strain Accumulation of the Lushan M_s7.0 Earthquake, as Reflected by GPS Surveying," *Chinese Science Bulletin*, **58**(20): 3460–3446.

Xu SG, Xiong YL, Liao H, *et al*. (2010), "Static and Kinematic Analysis of Coseismic Deformation of Wenchuan M_s8.0 Earthquake," *Journal of Geodesy and*

Geodynamics, **30**(3): 27–54. (in Chinese)

Yi GX, Yao HJ and Zhu JS (2008), "Rayleigh-wave Phase Velocity Distribution in China Continent and Its Adjacent Regions," *Chinese Journal of Geophysics*, **51**(2): 265–274. (in Chinese)

Yin HT, Gan WJ, Xiao GR, *et al*. (2009), "Progress on Monitoring Strong Earthquake Ground Motions Using High-rate GPS," *Progress in Geophysics*, 2**4**: 2012–2019. (in Chinese)

Yin HT, Zhang PZ, Gan WJ, *et al*. (2010), "Near-field Surface Movement during the Wenchuan M_s8.0 Earthquake Measured by High-rate GPS," *Chinese Science Bulletin*, **55**(23): 2529–2534.

Zhang XH, Guo F and Guo BF (2012), "Coseismic Displacement Monitoring and Wave Picking with High-frequency GPS," *Chinese Journal of Geophysics*, **55**(6): 1912–1918. (in Chinese)

Zumberge JF, Helfin MB, Jefferson DC, *et al*. (1997), "Precise Point Positioning for the Efficient and Robust Analysis of GPS Data from Large Networks," *J Geophys Res,* **102**(B3): 5005–5017.